

# Optimization of parameters in electron probe microanalysis

Rita Bonetto,<sup>1†</sup> Gustavo Castellano<sup>2\*</sup> and Jorge Trincavelli<sup>2†</sup>

<sup>1</sup> Centro de Investigación y Desarrollo de Procesos Catalíticos, CONICET–UNLP, Calle 47 No. 257, Cc 59, (1900) La Plata, Argentina

<sup>2</sup> Facultad de Matemática, Astronomía y Física, Universidad Nacional de Córdoba, Ciudad Universitaria, (5000) Córdoba, Argentina

Received 22 March 2000; Accepted 10 April 2001

A method for the refinement of atomic and experimental parameters applicable to several spectroscopic techniques is presented. This kind of procedure, previously used in x-ray diffraction, is shown to be a powerful tool in electron probe microanalysis (EPMA). This method consists of minimizing the differences between an experimental x-ray spectrum and a function proposed to account for the bremsstrahlung and characteristic peaks from the corresponding sample, and also for detection artifacts. This complicated function involves several parameters related to different sources (x-ray production, x-ray attenuation, sample composition, x-ray detection, etc.). Initial values must be supplied for them, and after a numerical iterative procedure is performed, improved values are achieved. Depending on the particular situation, certain parameters may be known *a priori*, so that they can be fixed, allowing the others to vary. In this way, the method can be used for different purposes: determination of atomic parameters such as fluorescence yields, transition rates or photoelectric cross-sections, quantitative standardless analysis, determination of detector characteristics, etc. This work is intended to present the general aspects of the method for refining EPMA parameters, and to give some examples of its application to the aforementioned issues. Even when only EPMA spectra are included in this work, the method can be applied to different spectroscopic techniques, such as x-ray fluorescence, particle-induced x-ray emission, etc. Copyright © 2001 John Wiley & Sons, Ltd.

## INTRODUCTION

Parameter refinement using the whole spectrum is a widespread technique in powder x-ray diffraction, and has widely been used in crystalline structural analysis. In this area, Rietveld<sup>1–3</sup> implemented the method for the first time. At present, the applications cover many different aspects, extending from the refinement of parameters in simple structures to more complicated situations, which include the refinement of parameters in complex structures, high-temperature superconductor structures, structural changes determined in real time, etc. (see, for example, Ref. 4 and references cited therein). As an additional important advantage, the method can be used for quantifying multiphase mixtures. However, the refinement methodology has not yet been extended to other spectroscopic techniques, such as electron probe microanalysis (EPMA) or x-ray fluorescence (XRF). In these areas, accuracy of different parameters is continuously searched for in order to improve the state of general scientific knowledge. To this end, interesting

results may be achieved by means of the optimization of atomic parameters that are poorly known, such as attenuation cross-sections for energies below 1.5 keV or, for ultra-light elements, atomic transition rates, fluorescence yields, etc.

On the other hand, since suitable standards for performing conventional analysis are not usually available, standardless analysis is always in continuous development. For this reason, the implementation of concentration refinement for standardless quantitation appears as an important tool in materials characterization.

The method presented here is devoted to the refinement of experimental and basic parameters which may not be accurately known. It is based on the theoretical prediction of characteristic and continuum intensities, allowing certain parameters to vary in order to obtain the best approach for the experimental spectrum. As a result, refined estimates for the sought parameters are achieved.

The algorithm consists in performing least-squares fitting of the entire observed spectrum. Although it may be applied to different spectroscopic techniques, this work is restricted to EPMA spectra acquired with an energy-dispersive system. An iterative procedure is carried out in order to minimize the differences between the experimental and the calculated spectra. The expressions used for the predicted spectrum are based on fundamental parameters for characteristic lines and bremsstrahlung emission, and take into account detection artifacts.

\*Correspondence to: G. Castellano, Facultad de Matemática, Astronomía y Física, Universidad Nacional de Córdoba, Ciudad Universitaria, (5000) Córdoba, Argentina.  
E-mail: gustavo@quechua.fis.uncor.edu  
†Consejo Nacional de Investigaciones Científicas y Técnicas de la República Argentina.  
Contract/grant sponsor: Consejo Nacional de Investigaciones Científicas y Tecnológicas de la República Argentina.  
Contract/grant sponsor: Secretaría de Ciencia y Técnica de la Universidad Nacional de Córdoba.

If  $I_i$  and  $\tilde{I}_i$  denote, respectively, the experimental and calculated intensities measured for the energy  $E_i$ , the quantity to be minimized can be written as

$$\chi^2 = \frac{1}{N-P} \sum_i \frac{(\tilde{I}_i - I_i)^2}{I_i} \quad (1)$$

where the summation runs over all  $N$  data points and  $P$  is the number of parameters adjusted. Thus,  $\chi^2$  will depend on the parameters to be optimized through the expressions chosen for  $\tilde{I}_i$ . Since these are complicated functions, the procedure involves a non-linear least-squares fitting, and the risk of falling in local minima is not negligible. In order to reduce this risk, the initial guess for the parameters must be fairly close to the correct values. An alternative way to overcome the problem is to begin with different estimates and check that the same minimum is achieved.

It is worth emphasizing that the procedure proposed here is devoted to the refinement or optimization of parameters, and it is not *per se* a method for determining them. Nevertheless, it may become a fundamental tool when associated with a quantitation routine. For example, as shown below, this procedure allows one to improve the mass concentrations given by the program MULTI<sup>5</sup> for standardless peak-to-background quantitation.

The outline of this paper is as follows: in next section, theoretical support is given for the prediction of whole spectra in EPMA, and a description is given of the method proposed for parameter optimization. Some applications are then presented; these include the characterization of detector properties, the refinement of atomic transition rates and the optimization of sample compositions. Finally, some conclusions are drawn, and a discussion about potential applications of the method is given.

## DEVELOPMENT OF THE METHOD

The structure of the method is supported on two different bases. On the one hand, a full theoretical description is given for spectra acquired in EPMA. On the other hand, a numerical procedure is used to minimize the differences between experimental and calculated spectra.

### Prediction of spectra

In order to predict a spectrum, a complete knowledge of the x-ray bremsstrahlung production, characteristic radiation emission and detection artifacts is required.

According to previous work,<sup>6</sup> the continuum spectrum corresponding to the emission of bremsstrahlung can be expressed as an analytical function of photon energy  $E$ , mean atomic number  $\bar{Z}$  and incident energy  $E_0$  of the electron beam impinging on the sample:

$$B = \alpha \sqrt{\bar{Z}} \frac{E_0 - E}{E} \left[ 54.86 - 1.072E + 0.2835E_0 + 30.4 \ln \bar{Z} + \frac{875}{Z^2 E_0^{0.08}} \right] AR \varepsilon \frac{\Delta\Omega}{4\pi} \quad (2)$$

where  $\alpha$  is a constant proportional to the number of incident electrons,  $A$  corrects for x-ray absorption,  $R$  takes into

account intensity losses due to electron backscattering,  $\varepsilon$  is the detector efficiency at energy  $E$  and  $\Delta\Omega$  is the solid angle subtended by the detector. This simple analytical function has shown very good performance for a wide set of experimental spectra as compared with other models.

The spectral peaks have a strong dependence on mass concentrations  $C$  and therefore they are the basis of any quantitative approach. The detected characteristic intensity  $P_{j,q}$  of the line  $q$  from element  $j$  in the sample can be written as<sup>7</sup>

$$P_{j,q} = \beta C_j (\mathbf{ZAF})_{j,q} Q_j \omega_j f_{j,q} \varepsilon_{j,q} \frac{\Delta\Omega}{4\pi} \quad (3)$$

where  $\beta$  is a constant proportional to the number of incident electrons,  $Z$ ,  $A$  and  $F$  are the atomic number, absorption and fluorescence matrix corrections, respectively,  $Q_j$  is the ionization cross-section for element  $j$  at energy  $E_0$ ,  $\omega_j$  is the fluorescence yield for the considered atomic (sub)shell and  $f_{j,q}$  is the transition rate related to the observed line  $q$ . The so-called **ZAF** corrections depend on the sample concentrations in a complicated way, and a number of different models has been proposed for them.<sup>8</sup> A description of the interaction between electrons and matter involving an ionization distribution function  $\phi(\rho z)$  with mass depth  $\rho z$  was considered for this work to account for both  $Z$  and  $A$  correction factors. Packwood and Brown's<sup>9</sup> description of  $\phi(\rho z)$  was taken as a basis for the more realistic model<sup>10</sup> used in the present method. The first applications of the method presented here do not include the  $F$  correction factor, since it is not very important in the samples studied. The fluorescence yield coefficients were taken from Hubbell,<sup>11</sup> whereas transition rates are usually optimized (see the next section).

Once bremsstrahlung and characteristic emission are taken into account, a number of effects produced during x-ray detection must be considered. In different x-ray analytical techniques, the most commonly used detectors are solid-state based, particularly lithium-drifted silicon [Si(Li)] detectors. For this kind of detector, the basic detection process involves a proportional conversion of photon energy into an electrical signal, which is shaped and amplified, and then passed to a multichannel analyzer. A relationship between the channel number in which photons are registered and the corresponding energy must be supplied. Usually, a linear calibration is implemented in the detection systems by means of two parameters, namely the *gain* and the *zero*. These two parameters depend on the detection chain settings, and they are known at least to a first approximation.

The detector system response for photons of energy  $E$  is a more or less broadened peak, whose distribution can be considered as Gaussian to a first approximation, its standard deviation  $\sigma$  being a function of photon energy:<sup>12</sup>

$$\sigma = (n^2 + \varepsilon FE)^{1/2} \quad (4)$$

where  $n$  is the uncertainty due to the electronic noise of the amplification process,  $F$  is the Fano factor and  $\varepsilon$  is the mean energy required for a single electron-hole pair formation, which in Si(Li) detectors at 77 K is 3.76 eV.

Another important feature of the registered spectrum which must be accounted for is the detector efficiency. In

an Si(Li) detector, the efficiency is close to 100% above 3 keV, but falls at lower energies owing to absorption in the isolation window and front layers. Typically, three different thicknesses must be known: a thickness specific to the window (usually made of beryllium), a gold layer contact evaporated on to the front surface and a dead silicon layer.

An additional artifact of spectra collected with Si(Li) detectors is a spurious Si peak due to the photoelectric absorption of the photon to be detected, within the dead Si layer of the detector. When this process occurs, the Si K photon may enter the active region and be registered, whereas Auger and photoelectrons are much more likely to be absorbed in the dead layer.<sup>13</sup> As a result, a photon of only 1.739 keV, corresponding to the Si K peak is registered instead of the one actually emitted by the sample. The height of this spurious peak is difficult to estimate and it may lead to a wrong quantitation when silicon is present in the sample.

Finally, some of the charge carriers produced by a photon arriving at the detector may be 'trapped' before being collected. Thus, the output sent to the amplifier corresponds to an energy lower than the original value. This effect is manifested in asymmetric peaks with low-energy tails, departing from the assumed Gaussian shape. Since the highest concentration of traps occurs in a transient region close to the detector surface, between the active volume and the dead layer, peaks appear to be more asymmetric for soft x-ray lines. Therefore, a modification to the Gaussian function is necessary in order to account for this effect.

There are two further artifacts which have not been considered in this first stage, since they would not influence the results. First, there is a finite probability that Si K photons produced in the detector following absorption of an incident photon will escape from the detector. In this event, the energy of the escape photon is not deposited in the detector, and the height of the consequent pulse is correspondingly reduced, i.e. an 'escape peak' occurs 1.739 keV below the main peak. Second, two pulses may reach the main amplifier within a very short time interval, resulting in the appearance of a spurious peak in the spectrum, corresponding to the sum of the energy of the two original pulses.

### Optimization of parameters

The functional behaviour of the whole spectrum can be achieved following the description of the previous paragraphs. However, some parameters may not be precisely known *a priori*; the challenge is therefore to find the set of parameters which best fits the general shape of the proposed function to the experimental spectrum:

$$\tilde{I}_i = B(E_i) + \sum_{j,q} P_{j,q} H_{j,q}(E_i) + P_{\text{Si}} G_{\text{Si}}(E_i) \quad (5)$$

where  $E_i = \text{zero} + i \cdot \text{gain}$  is the energy corresponding to channel  $i$ ,  $H_{j,q}$  is a modified Gaussian function (see below) associated with the peak intensity  $P_{j,q}$  and  $P_{\text{Si}}$  is the internal fluorescent Si peak, spread by means of a Gaussian distribution  $G_{\text{Si}}$ . The parameters which may be optimized are: the scaling factors  $\alpha$  and  $\beta$  of Eqns (2) and (3), the *zero* and *gain* of the detection chain, the peak-width factors  $n$

and  $F$  of Eqn (4), the transition rates  $f_{j,q}$ , the fluorescence yields  $\omega_j$  and the mass concentrations  $C_j$  of Eqn (3), the three parameters involved in the function  $H_{j,q}$  for each peak, the three thicknesses associated with the detector efficiency, the amplitude of the  $P_{\text{Si}}$  peak, the transition energies for the involved decays, etc.

Since  $\tilde{I}_i$  of Eqn (5) is involved in Eqn (1), the algebraic complexity of the expression for  $\chi^2$  requires a numerical procedure for its minimization. Even when no perfect minimization procedure exists, certain characteristics of a given routine make it suitable for a particular application. Among the different possibilities (see, e.g., Ref. 14), the downhill simplex algorithm<sup>15</sup> was chosen because, in addition to being a robust routine, it requires only function evaluations, not derivatives. This fact is particularly important since it is often necessary to deal with functions whose computed derivatives do not accurately point the way to the minimum, usually because of truncation error in the method of derivative evaluation.

It must be kept in mind that minimization methods can lead to a local minimum instead of the desired global minimum. A good way to overcome this problem is to start from a reasonable initial guess for the parameters to be optimized; in addition, it is frequently a good idea to restart the minimization routine at the point where it claims to have found the minimum, reinitializing certain ancillary scale factors.<sup>14</sup> Another solution for confirming that the minimum found is the global one is to try to obtain it by starting from widely varying initial values for the parameters.

Usually, it is helpful to carry out the procedure by choosing one or two parameters at a time; once their values have been achieved, they are set fixed and other reduced group of parameters is allowed to vary. When all the chosen parameters are refined, the procedure may be restarted with the obtained values as initial guesses, varying all of them simultaneously. Sometimes, a visual examination of the intermediate results is required in order to make an appropriate decision for the strategy to adopt. For this purpose, it is useful to plot the predicted and experimental spectra, in addition to their differences, after the criterion of convergence is fulfilled.

The optimization method described above was implemented in the computer program POEMA (parameter optimization in electron microprobe analysis). The applications shown in next section were carried out by means of this program.

### SOME APPLICATIONS

In order to demonstrate the capabilities of the proposed method, several spectra of standard samples were used, measured in a CAMECA SX-50 microprobe with an Si(Li) detector. Non-conductive samples were coated with a thin carbon layer in order to avoid charge accumulation and heating. Depending on the parameter to be refined, different spectral regions were considered, since the influence of each parameter shows up at different energy ranges.

The program developed allows one to modify the input file, in order to choose the parameters to be optimized.

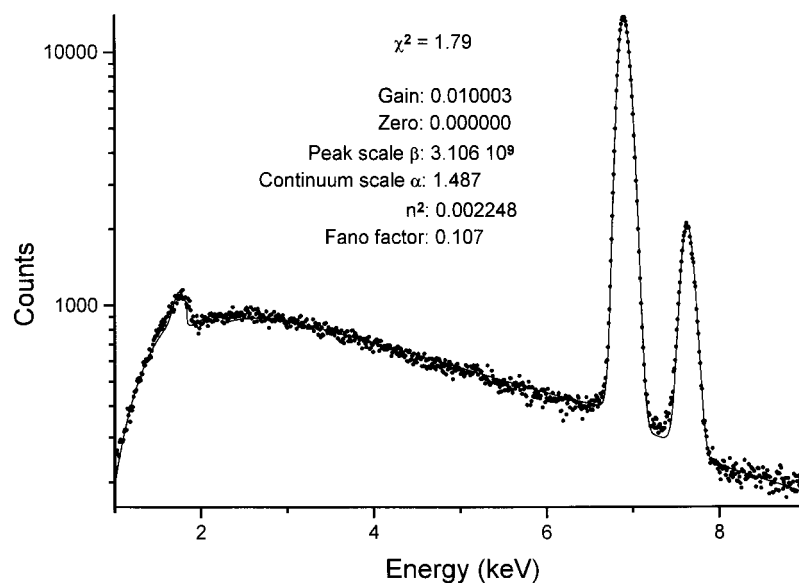


**Figure 1.** Fit for a pure Co spectrum irradiated at 20 keV. Dots, experimental; solid curve, fitted spectrum. The values for the refined parameters are also shown.

As explained above, the best choice is to begin with the refinement of a few parameters; for the examples presented below, the first refinement is always performed on the overall scale factors  $\alpha$  and  $\beta$  for the continuum spectrum and the characteristic lines, respectively. Typically, after this first step, an additional refinement of the calibration and detector response parameters is necessary, particularly when the experimental conditions are changed. As an example, Fig. 1 shows the spectrum fitted for a pure cobalt sample, and the set of optimized parameters. A logarithmic scale is used in this and next plots, in order to emphasize relative differences between experimental and predicted values. For this case, the value for the transition rate was taken from Salem.<sup>16</sup> As can be seen, the whole predicted spectrum shows very good agreement with experimental data, with  $\chi^2 = 1.79$ . The Fano factor achieved is in agreement with typical values.<sup>17</sup> The good performance of this application of the method implies that the models used for the different processes involved are correct, especially those related to the generation and absorption of bremsstrahlung and fluorescent lines.

## Detector characteristics

### Detector thicknesses

As mentioned above, three thicknesses must be supplied in order to know the detector efficiency at low photon energies (<3 keV). These thicknesses are usually provided by the detector manufacturer, but their values may change with time owing to different reasons. The beryllium window often becomes stained, usually because of the presence of oil molecules coming from the vacuum pump. On the other hand, the cooling system may favour the nucleation of water molecules, resulting in the growth of ice crystals on the gold surface layer. Finally, the dead silicon layer may be modified because of the migration of lithium atoms within the crystal. Since it is very difficult to measure each of these thicknesses, the method of parameter optimization is proposed as a tool to solve this problem.

**Table 1.** Characteristic detector thicknesses determined by using four pure samples

Sample	Be ( $10^{-4}$ cm)	Au ( $10^{-6}$ cm)	Si ( $10^{-5}$ cm)
Ti	9.6	1.9	2.9
V	9.1	2.1	2.9
Mn	9.0	1.6	2.7
Co	8.9	2.0	2.5
Average	9.2	1.9	2.8

For the sake of simplicity, each thickness is assumed to remain mono-elemental after contamination. Bearing this hypothesis in mind, the efficiency curve of an Si(Li) detector at low energies was characterized. The 'effective' thicknesses were optimized by using four different pure samples. According to the results shown in Table 1, reasonable values were found, showing an acceptable agreement among the different samples used. The mean values obtained for each thickness were used for all the spectra fitted in the present work.

### Internal fluorescent peak

As can be seen from Fig. 1, a small peak appears below 2 keV. This spurious Si peak has been mentioned above as inherent to the detection process. Its height is difficult to predict because it depends in a complicated way on the detector geometry and on the photon spectrum itself. For this reason, it is a parameter typically refinable by the optimization process, starting from an initial value estimated by visual observation of the spectrum. When silicon is present in the sample, it is necessary to determine previously the internal fluorescent peak height in a sample of similar composition, but without silicon. The good fit achieved for the Si peak illustrated in Fig. 1 shows the usefulness of the method for this application.

### Incomplete charge collection

As explained above, when not all charge carriers reach the detector electrodes, a reduction in the registered pulse height results in 'tailing' in the low-energy side of the peak. For this reason, an asymmetric correction to the ideal Gaussian peak is required. In the present work, the Hypermet<sup>18</sup> function was chosen:

$$H_{j,q}(E_i) = M[G_{j,q}(E_i) + S_{j,q}(E_i) + T_{j,q}(E_i)]$$

where  $M$  is a normalization factor,  $G_{j,q}(E_i)$  is a Gaussian function centred at the characteristic energy  $E_{j,q}$ :

$$G_{j,q}(E_i) = \frac{1}{\sqrt{2\pi}\sigma_{j,q}} \exp\left[-\frac{(E_i - E_{j,q})^2}{2\sigma_{j,q}^2}\right]$$

$S_{j,q}(E_i)$  is the step function of height  $s_{j,q}$  convoluted by the Gaussian:

$$S_{j,q}(E_i) = s_{j,q} \operatorname{erfc}\left(\frac{E_i - E_{j,q}}{\sqrt{2}\sigma_{j,q}}\right)$$

and  $T_{j,q}(E_i)$  is an exponential tail of width  $\beta_{j,q}$  and height  $t_{j,q}$  convoluted by the Gaussian:

$$T_{j,q}(E_i) = t_{j,q} e^{(E_i - E_{j,q})/\beta_{j,q}} \operatorname{erfc}\left(\frac{E_i - E_{j,q}}{\sqrt{2}\sigma_{j,q}} + \frac{\sigma_{j,q}}{\sqrt{2}\beta_{j,q}}\right)$$

In these functions, the parameters  $s_{j,q}$ ,  $t_{j,q}$  and  $\beta$  are not known *a priori* and must be refined if peak asymmetries are taken into account. Figure 2 shows a clear example in which peak-shape corrections for Ca K-lines are unavoidable in a dolomite sample.

### Transition rates

Inner shell transition probabilities have been dealt with extensively. The reason why special attention has been paid to transition rates is mainly because reliable experimental values can be used as a straight test for theoretical atomic

models. In particular, separate relativistic Hartree–Fock solutions for atoms in their initial and final states have been used for calculating radiative decays of K or L vacancy states.<sup>19,20</sup> On the other hand, spectroscopic techniques based on x-ray emission analysis have largely evolved in recent decades. This is mainly due to its non-destructive nature, which permits the reproducibility of results, and to the low detection limits achieved (ppm and ppb levels). An adequate knowledge of transition rates allows the analyses to be improved, since peak overlaps between e.g.  $K\alpha$  and  $K\beta$  lines of neighbouring elements are frequently a problem for the analyst.

The spectra selected for this example were first fitted to find adequate values for scale factors and detector response, as explained above. Once the proper values for these parameters have been achieved, they are fixed and the line fractions are refined instead. In this particular case, it is convenient to perform the refinement along with the peak scale factor  $\beta$  of Eqn (3), since changes in the intensity ratios may influence its value.

The values obtained for transition rates are compared with theoretical<sup>19</sup> and experimental<sup>21</sup> data from the literature in Table 2. These line fractions are taken as the ratios between  $K\alpha$  intensities and total K ( $K\alpha + K\beta$ ) intensities. As can be seen, good agreement is achieved, following the general trend of experimental and theoretical data.

The good performance of this method for K ratios encourages the study of relative transitions involving decays to different inner atomic shells, for which measurements and theoretical predictions are more difficult.

### Sample composition

Most analytical techniques are based on the determination of characteristic intensities detected from the sample of interest and from reference standards. The method presented here allows the refinement of concentrations in the irradiated material by means of the best fit of a unique spectrum. With the purpose of showing the capabilities of this method in this

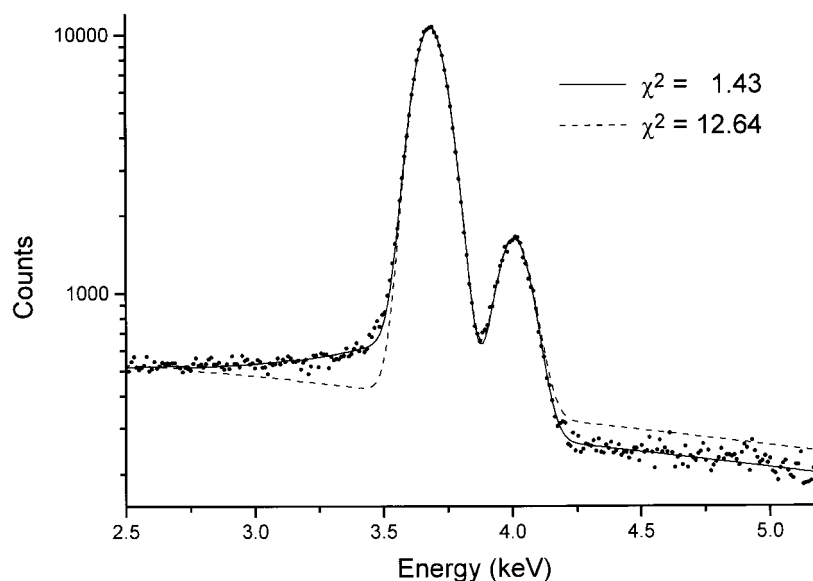


**Figure 2.** Spectral region including Ca K-lines fitted for a dolomite sample. Dots, experimental; dashed curve, best fit using a Gaussian distribution for the peaks; solid curve, best fit using the Hypermet function.

**Table 2.** Transition rates for K decays determined by the method proposed in this work compared with values from the literature

Element	This work	Ref. 19	Ref. 21
Ca	0.890	0.884	0.887
Ti	0.886	0.881	0.884
V	0.883	0.880	0.883
Cr	0.883	0.882	0.883
Fe (in siderite)	0.884	0.878	0.882
Co	0.880	—	0.881

kind of application, several samples of known composition were analyzed.

The first example involves a cobalt oxide, for which nominal mass concentrations are 78.65% Co and 21.35% O. Despite its simplicity, this is a very interesting situation, since neither a characteristic peak is observed for oxygen nor are standards used. In addition, the stoichiometric relationship is assumed to be unknown, although the information that there is no further element is taken into account by normalizing to 100%. As mentioned above, initial values for the parameters should not be too different from the correct ones, since the risk of falling in local minima for  $\chi^2$  must be avoided. Nevertheless, in this case the respective initial values were set as 83 and 17%, rather different from the true values. The strategy followed was to refine only the cobalt concentration and the overall scale factors. After a first iteration, both concentrations were renormalized to 100% and used as input for a further iteration. This strategy was repeated until convergence. The final values achieved were 78.14% Co and 21.86% O, which are in very good agreement with the nominal composition.

The next specimen considered is a siderite sample, whose nominal concentrations are shown in Table 3. In this case, the specimen composition was first estimated by means of the standardless peak-to-background algorithm of Trincavelli

**Table 3.** Mass concentrations (%) calculated by the program MULTI and optimized by this work, as compared with nominal values for a siderite sample

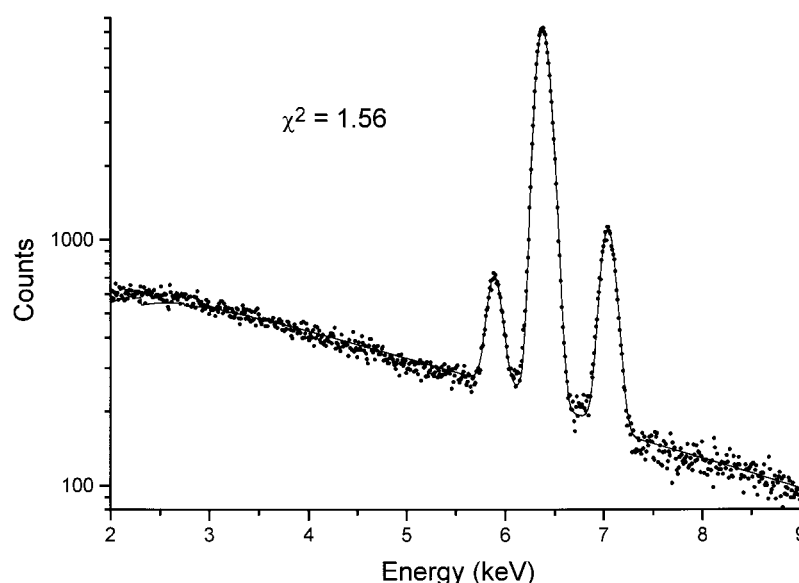
Element	MULTI	This work	Nominal
Fe	46.35	45.36	45.93
Mn	2.98	2.27	2.28
O	40.71	42.08	41.45
C	9.96	10.29	10.34

and Van Grieken,<sup>7</sup> as included in program MULTI;<sup>5</sup> to this end, stoichiometric relationships were considered for determining carbon and oxygen. For the refinement of concentrations by means of the method presented here, normalization to 100% was used as in the previous example. The good fit achieved for this example is shown in Fig. 3. As can be observed, the problem of peak overlapping is adequately overcome, in this case Mn K $\beta$  and Fe K $\alpha$ . Table 3 shows how the good estimates obtained by means of MULTI are improved, particularly for minor elements.

It is worth noting that when the input values are very close to the nominal concentrations, the stability of the method must hold. This condition is fulfilled only if a good theoretical description of the whole spectrum is given and a robust numerical minimization routine is provided. This is illustrated in Table 4, in which a dolomite sample is

**Table 4.** Mass concentrations (%) calculated by the program MULTI and optimized by this work, as compared with nominal values for a dolomite sample

Element	MULTI	This work	Nominal
Ca	21.63	21.68	21.75
Mg	13.58	13.56	13.13
O	51.82	51.75	52.12
C	12.96	12.94	12.93

**Figure 3.** Spectral region fitted for a siderite sample. Dots, experimental; solid curve, fitted spectrum.

characterized: the predictions given by the program MULTI are very good and, consequently, the present method slightly improves them.

## CONCLUSIONS

A versatile method for parameter optimization has been presented, which allows the refinement of different magnitudes of interest in the frame of atomic physics and also analytical and physical chemistry. Although in this work only EPMA spectra were used, the scope of the proposed method includes other spectroscopic techniques, such as x-ray fluorescence, particle induced x-ray emission, etc., for which the corresponding theoretical description should be supplied.

An important feature of this methodology is the capability of refining atomic parameters such as radiative decay rates, Coster–Kronig yields, fluorescence yields, mass attenuation coefficients for low photon energies, etc. Some examples of K-shell transition rate refinement have been given here, showing a very good performance. In view of these results, work is being done on the study of L-shell transition rates. Additional applications may be carried out in the refinement of some of the parameters involved in modelling characteristic lines and bremsstrahlung spectrum. Alternatively, the effect of chemical bonds on transition rates and energies can also be investigated by means of the procedure of parameter optimization proposed.

The method implemented in this work achieves a very good description of whole spectra in electron probe microanalysis. The good performance shown in the examples given above, with  $\chi^2$  values  $<2$ , is reflected in values for the parameters optimized that are very close to the corresponding expected values. This suggests that the methodology proposed here may become a powerful tool for the refinement of fundamental atomic magnitudes,

and also an essential stage for standardless quantitation routines.

## Acknowledgements

The authors thank Professor J. A. Riveros for kindly reviewing the manuscript. Special acknowledgement is due to Professor Marcos Vasconcellos (Universidade Federal do Rio Grande do Sul) for his invaluable contribution to the experimental spectra. This work was partially supported by the Consejo Nacional de Investigaciones Científicas y Tecnológicas de la República Argentina and the Secretaría de Ciencia y Técnica de la Universidad Nacional de Córdoba.

## REFERENCES

1. Rietveld H. *Acta Crystallogr.* 1966; **20**: 508.
2. Rietveld H. *Acta Crystallogr.* 1967; **22**: 151.
3. Rietveld H. J. *Appl. Crystallogr.* 1969; **2**: 65.
4. Young R. *The Rietveld Method*. International Union of Crystallography, Oxford University Press: Oxford, 1993.
5. Trincavelli J, Castellano G. *X-Ray Spectrom.* 1999; **28**: 194.
6. Trincavelli J, Castellano G, Riveros JA. *X-Ray Spectrom.* 1998; **27**: 81.
7. Trincavelli J, Van Grieken R. *X-Ray Spectrom.* 1994; **23**: 254.
8. Riveros J, Castellano G. *X-Ray Spectrom.* 1993; **22**: 3.
9. Packwood R, Brown J. *X-Ray Spectrom.* 1981; **10**: 138.
10. Riveros J, Castellano G, Trincavelli J. *Mikrochim. Acta (Suppl.)* 1992; **12**: 99.
11. Hubbell J. NISTIR 89–4144. Gaithersburg, MD: National Institute of Standards and Technology, 1989.
12. Goldstein J, Newbury D, Echlin P, Joy D, Romig A Jr, Lyman C, Fiori C, Lifshin E. *Scanning Electron Microscopy and X-Ray Microanalysis*, (2nd edn). Plenum Press: New York, 1992.
13. Reed S. *Electron Probe Microanalysis* (2nd edn). Cambridge University Press: Cambridge, 1993.
14. Press W, Flannery B, Teukolsky S, Vetterling W. *Numerical Recipes*. Cambridge University Press: Cambridge, 1989.
15. Nelder J, Mead R. *Comput. J.* 1965; **7**: 308.
16. Salem S. *Phys. Rev. A* 1972; **6**: 2147.
17. Knoll G. *Radiation Detection and Measurement* (2nd edn). John Wiley & Sons: New York, 1989.
18. Phillips G, Marlow K. *Nucl. Instrum. Methods* 1976; **137**: 525.
19. Scofield J. *Phys. Rev. A* 1974; **9**: 1041.
20. Scofield J. *Phys. Rev. A* 1974; **10**: 1507.
21. Khan Md. R, Karimi M. *X-Ray Spectrom.* 1980; **9**: 32.